Phys. Status Solidi A **211,** No. 6, 1340–1345 (2014) / **DOI** 10.1002/pssa.201330376

Part of Special Issue on
Engineering of Functional Interfaces

physica status solidi a
www.pss-a.com
applications and materials science

On the pH-sensing properties of differently prepared tungsten oxide filmsol

Stefanie Drensler[1], Sarah Walkner[1,2], Cezarina Cela Mardare[3], and Achim Walter Hassel[*,1,2,3]

[1] Institute for Chemical Technology of Inorganic Materials, Johannes Kepler University Linz, Altenberger Str. 69, 4040 Linz, Austria
[2] Competence Centre for Electrochemical Surface Technology, Viktor Kaplan Str. 2, 2700 Wiener Neustadt, Austria
[3] Christian Doppler Laboratory for Combinatorial Oxide Chemistry at the Institute for Chemical Technology of Inorganic Materials, Johannes Kepler University Linz, Altenberger Str. 69, 4040 Linz, Austria

Received 19 October 2013, revised 17 December 2013, accepted 15 January 2014
Published online 7 February 2014

Keywords microelectrodes, pH sensors, tungsten, WO_3

* Corresponding author: e-mail achimwalter.hassel@jku.at, Phone: +43 732 2468 8701, Fax: +43 732 2468 8905

In this paper, different preparation routes and designs for pH sensing metal/metal oxide electrodes are evaluated. Crystallographic changes in the oxide film are responsible for the pH-sensing capability of tungsten oxide. As the present oxide structure is directly limiting the measuring range, as-received tungsten oxide powders were heat treated to produce polymorphs of WO_3, in an attempt to extend the measuring range. Furthermore, electrochemical oxide covered electrodes ranging from micro- down to nano-dimensions have been implemented. Optional coating with Nafion, serving as a membrane material, allows shifting the measuring range even to strongly alkaline conditions.

1 Introduction In both industrial and laboratory use, pH is commonly measured using commercial glass electrode techniques as they combine a high stability with a wide measuring range. According to the experimental demands specialized electrodes, like yttria-stabilized zirconia (YSZ) membrane electrodes and hydrogen electrodes for measurements in high-temperature environments [1, 2] have been implemented. Also ion-selective field effect transistors (ISFETs) for small electrolyte volumes [3, 4] and even localized pH-measurements using micro-capillaries have been developed [5]. One promising material meeting the experimental demands for an application at elevated temperatures requiring only a minimum volume of test solution, is the tungsten/tungsten oxide system. The pH-sensing capability of tungsten oxide was already discovered in 1923 by Baylis [6] who monitored the pH during water purification using an ordinary light bulb connected to a calomel reference electrode (RE). Only a limited number of other metal oxides like platinum, palladium, ruthenium or iridium oxide, are suitable for pH sensing [7].

In recent years several authors applied tungsten/tungsten oxide electrodes for pH monitoring. Macdonald et al. [8] used thermally oxidized tungsten-wires to measure the pH during emulsion polymerization in a high-pressure atmosphere at elevated temperatures. Also for measurements in endothelial cells, as shown by Yamamoto et al. [9], tapered tungsten ultra-microelectrodes were used.

In this work, the influence of the crystallographic structure of tungsten oxide powders onto the pH sensitivity is evaluated. Based on these findings tungsten oxide micro- and nano-electrodes were fabricated using two different approaches allowing a drastic minimization of the required test solution volume.

2 Experimental

2.1 Production of macroscopic WO_3 films WO_3 powder (Wolfram Bergbau und Hütten AG) was heat treated in air for 10 h at different temperatures. The cooling was performed at different rates (Table 1) in order to stabilize the above room temperature WO_3 polymorphs: low-temperature monoclinic (from −140 to −50 °C), triclinic (from −50 to 17 °C), room-temperature monoclinic structure (17–330 °C), orthorhombic (330–740 °C), or tetragonal at temperatures higher than 740 °C [10, 11].

XRD measurements were performed using a Philips X'Pert PRO diffractometer with Cu K_α radiation and working in Bragg–Brentano geometry. The surface investigation of the powders and prepared samples was done using a field emission scanning electron microscope (SEM, Zeiss LEO 1540XB).

Table 1 Substrate with corresponding heat treatment and cooling procedures.

sample name	T (°C)	cooling (K min^{-1})
WO_3 – 0	–	–
WO_3 – 1	275	10
WO_3 – 2	500	10
WO_3 – 2′	500	withdrawn rapidly from the furnace to ambient temperature
WO_3 – 3	600	quenched in liquid N_2
WO_3 – 4	750	10

A suspension of the WO_3 powder and 1 wt% Nafion (persulfonic acid; Alfa Aesar, Karlsruhe, Germany) in a ratio of 1:20 was produced. Small suspension spots were dropped on a copper plate (Alfa Aesar) and subsequently dried in air. A Ag/AgCl micro-RE was prepared by electrochemical deposition of AgCl in a 1 M HCl onto a 100 μm thick Ag wire (Wieland Dentaltechnik, Pforzheim, Germany).

The wire was subsequently placed inside a glass capillary with an outer diameter of 500 μm (Hilgenberg GmbH, Malsfeld, Germany) and was filled with an agar-gelled 3 M KCl solution. A further description of the preparation procedure for Ag/AgCl micro-REs can be found elsewhere [12]. To test the dried spots of WO_3/Nafion suspensions on their pH-sensing properties the RE was placed into a bigger capillary with 2.5 mm outer diameter and an electrolyte inlet for different buffer solutions. The sample was contacted with a small electrolyte droplet formed at the very tip of the outer capillary as shown in Fig. 1.

2.2 Production of the micro pH electrode For the preparation of the oxide micro-electrodes a tungsten wire (99.95%, Alfa Aesar) with 100 μm diameter was inserted into a glass capillary which was afterwards filled with epoxy resin. Then the electrode was ground with 4000 grit emery paper, cleaned with acetone and water in an ultrasonic bath to obtain a defined circular surface. The WO_3 layer was produced electrochemically. Therefore, the micro-electrode was immersed in 2 M H_2SO_4 and cycled between +1 V (SHE) and +2 V (SHE) for 20 cycles with a scan rate of 20 mV s^{-1} using a dimensionally stable anode (DSA) (Metakem, Usingen, Germany) as counter electrode (CE) and a commercial Ag/AgCl RE (Metrohm, Filderstadt, Germany). The micro-electrode was then immersed into 2 M H_2SO_4 for 12 h and stored in 0.5 M H_2SO_4 until further use.

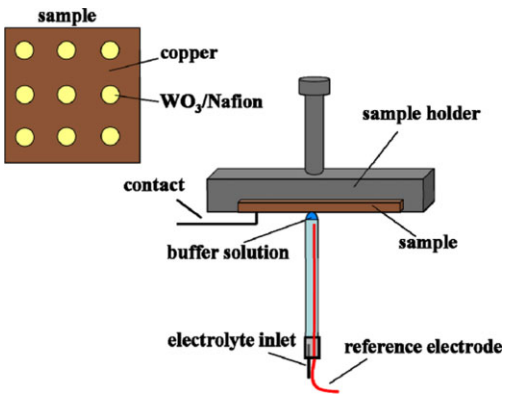

Figure 1 Setup for the electrochemical measurements of the WO_3/Nafion suspensions.

2.3 Tungsten nanowires for pH sensing Prior to the directional solidification process, master alloys with 1.5 at% W and an equiatomic ratio of both Ni and Al were prepared. The master alloys were induction molten and subsequently cast into a cylindrical, water-cooled copper mould. Directional solidification of the alloys was performed in a Bridgman furnace with a temperature gradient of 40 K cm^{-1} and a withdrawal rate of 200 mm h^{-1}. The specimens were then cut into disc shape and mechanically ground and diamond polished up to a final grade of 3 μm.

Scanning droplet cell microscopy (SDCM) was utilized to expose arrays of tungsten nanowires (further termed nano-electrode) from the surrounding NiAl-matrix. Therefore, a glass capillary with an outer diameter of 2.5 mm (Hilgenberg GmbH) was thermally tapered using a capillary puller (PC-10, Narishige, Tokyo, Japan) and ground using an in-house built capillary grinder with grade 2400 SiC paper. The capillary tip was then dipped into silicone (RTV 118Q, Momentive, Albany, USA) and dried for several hours under nitrogen flow. The gasket formation ensures a reproducibly wetted area of the sample in the contact mode with an average diameter of 713 μm (calculated from eight different spots) and is additionally preventing a cell leakage caused by hydrogen evolution occurring at the CE during matrix dissolution.

The CE consists of a 100 μm thick spiral gold wire (purity 99.999%, Wieland Dentaltechnik), which was wound around a before prepared micro-RE. Both CE and RE were inserted into the glass capillary and fixed together with a syringe needle of 500 μm diameter as electrolyte inlet using two-component adhesive glue. A schematic view of the used SDCM setup is shown in Fig. 2.

2.4 Electrochemical test procedures The electrochemical conditions for the dissolution of the NiAl-matrix can be derived from the combined Pourbaix diagrams of all three involved elements Ni, Al, and W. Hence, the dissolution of both Ni and Al is possible while W is passivated [13]. Therefore, a potential of 250 mV in 1 M HCl was chosen for a duration of 300 s. All electrochemical experiments were carried out using a Compactstat potentiostat (Ivium Technologies, Eindhoven, The Netherlands) or an EmStat Potentiostat (PalmSens, Utrecht, The Netherlands).

To determine the pH dependency of the potential for all three prepared oxides, the open circuit potential (OCP) was measured after an equilibration time of 500 s. Therefore buffer solutions from 0.1 M citric acid and 0.2 M di-sodium hydrogen phosphate [14] with a pH ranging from 3.00 up to

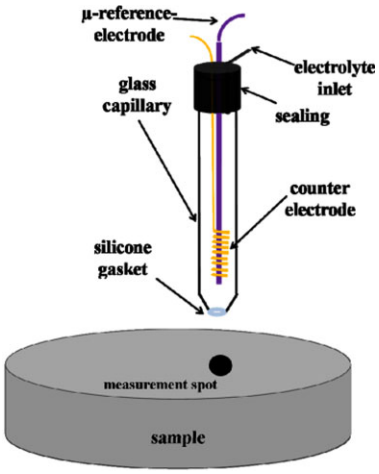

Figure 2 Schematic view onto the SDCM setup used for the small spot dissolution of directionally solidified NiAl–W.

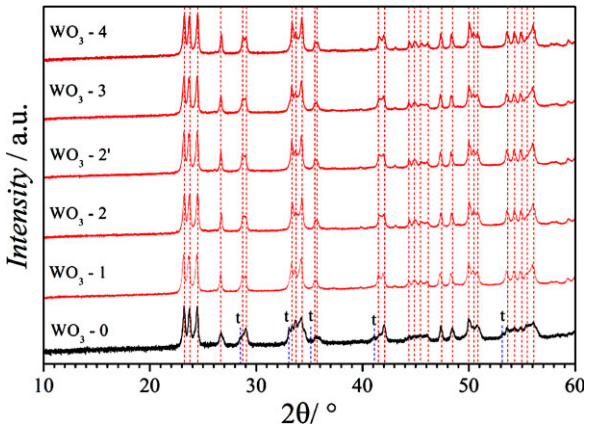

Figure 3 X-ray diffractograms of differently heat treated WO_3-powders, which show either a mixture of triclinic and monoclinic phases (WO_3 – 0) or only monoclinic phase (WO_3 – 1, WO_3 – 2, WO_3 – 3, WO_3 – 4).

7.00 were prepared. In addition, commercial buffer solutions from DM Messtechnik (Seeon, Germany) and Merck (Darmstadt, Germany) were used.

Prior to each measurement the pH of each solution was tested using a WTW inoLab pH-Meter equipped with a commercial glass electrode.

3 Results and discussion

3.1 Crystallographic structure and pH dependency The pH sensing property of tungsten oxide is based on the following reaction:

$$WO_3 + xH^x + xe^- \leftrightarrow H_xWO_3 \quad (0 < x < 1). \qquad (1)$$

If x equals to 0, the structure of the layer forms a ReO_3-type. Higher x values lead to a defect perovskite structure, and for $x = 1$ a perovskite structure is obtained [15].

Thus, the crystal structure of the as-received powder was investigated using X-ray diffraction. The powder diffractogram (WO_3 – 0) shows a mixture of triclinic and room-temperature monoclinic phases (Fig. 3). The peak positions from monoclinic and triclinic phases differ just slightly, but the triclinic phase possesses a few more peaks (indicated by t in Fig. 3), which can be clearly observed in the diffractogram ($2\theta = 28.4^\circ$, 33.07°, 35.02°, 41.1°, and 53.1°). These diffraction peaks are closely matching the reference pattern PDF# 00-020-1323 of the triclinic WO_3 and do not belong to the monoclinic WO_3 (PDF# 01-083-0950).

For an extension of the pH range, a combination of different oxide structures especially with the orthorhombic structure would be desirable. Independent of the heat treatment temperature and the cooling method, the rest of the powders (WO_3 – 1 to WO_3 – 4) showed only the presence of the monoclinic phase (Fig. 3), suggesting that upon cooling the higher temperature phases are converted back to the room-temperature stable phase (monoclinic).

After drying the suspension of both the as-received WO_3 powder and the purely monoclinic WO_3 with Nafion, the pH–potential-dependency in different electrolyte solutions was tested. SEM investigation of the dried suspension spots on the copper substrate, shown in Fig. 4, prove a full coverage which ensures that the potential is measured at the tungsten oxide/electrolyte interface.

For the monoclinic structure, a Nernstian behavior could only be found between pH 1.80 and 5.00. However, for the mixture of monoclinic and triclinic oxides the measuring range could be extended to 6.58 as shown in Fig. 5.

The fact that the measurable pH-range in the case of the monoclinic oxide is rather limited, can directly be explained by the crystallographic structure. Due to space limitations of the lattice the protons can only be intercalated into the oxide layer up to a certain extent.

Electrochemical oxidation of pure tungsten as an alternative way for the production of WO_3 offers the opportunity for a layer-by-layer oxide formation with an eventually different crystallographic structure.

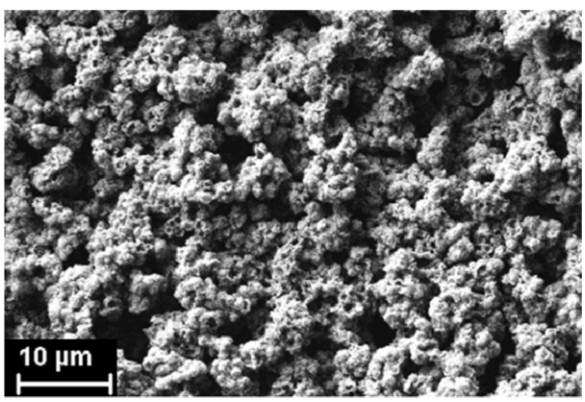

Figure 4 SEM image of the prepared WO_3/Nafion film on copper after drying.

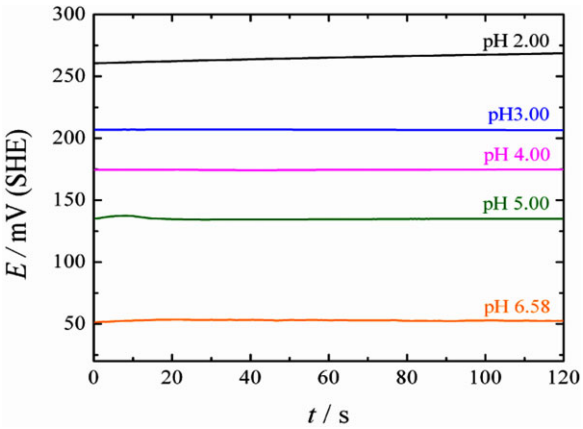

Figure 5 Time–potential dependency at different pH values of the WO_3/Nafion suspension.

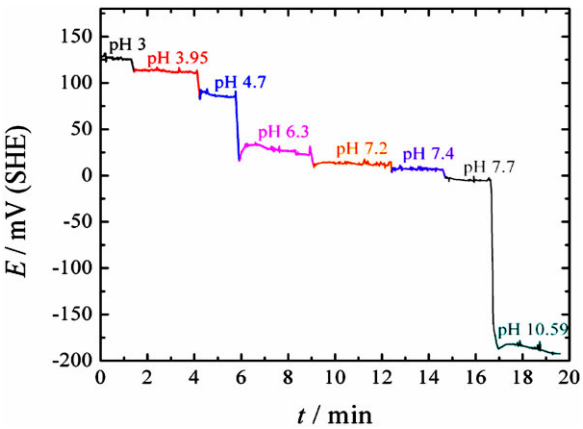

Figure 7 Titration curve obtained during a titration of HCl with NaOH and the prepared micro-electrode as pH-electrode.

3.2 Electrochemically grown tungsten oxide On both electrode types prepared – micro- and nano-electrodes – oxides were grown electrochemically. Electrochemical oxidation through a series of cyclic voltammograms allows a layer-by-layer oxide growth on the micro-electrode surface. A comparison of the sensitivity range to the suspensions used before, showed an increase in the measuring range from pH 1.00 to 7.00 (Fig. 6a) for the prepared micro-electrodes.

An advantage of this type of metal/metal oxide electrodes is the short response time of the system as demonstrated by a titration of HCl with NaOH (Fig. 7).

Especially the fast response to drastic pH changes (from 7.7 to 10.9) within less than 3 s makes this type of electrode an interesting alternative were commercial glass electrodes cannot be applied. Even an extension into the alkaline region, as shown in the titration curve is possible although longer exposure times to alkaline solutions have to be avoided due to the fact that WO_3 is transforming into WO_4^{2-} and thus the electrode is losing its pH sensitivity.

Another advantage of the used pH-microelectrodes is the possibility of measuring pH in very small electrolyte volumes of $<10\,\mu l$. Nevertheless, a further volume decrease can only be reached by scaling down also the electrode dimensions on which the oxide is grown. Hence, tungsten nanowire electrodes were produced through directional solidification of a pseudobinary eutectic NiAl–W alloy. A detailed description of the solidification method, effect of growth parameters and the underlying mechanism can be found elsewhere [16]. An additional electrochemical dissolution step is required to both locally and selectively dissolve Ni and Al while passivating W [17], thus, creating inherently the pH sensitive layer. The usage of SDCM allows creating cavities with W nanowires protruding from the matrix material (Fig. 8a) with a defined reproducible diameter as depicted in Fig. 8b.

Nano-electrodes solely show a pH–potential dependency from pH 4.00 to 7.00. The corresponding pH–potential diagram is shown in Fig. 6b. The measurable pH range is in particular limited to a minimum of pH 4.00 by the stability range of the present Al_2O_3 oxide layer protecting the NiAl-matrix from further dissolution.

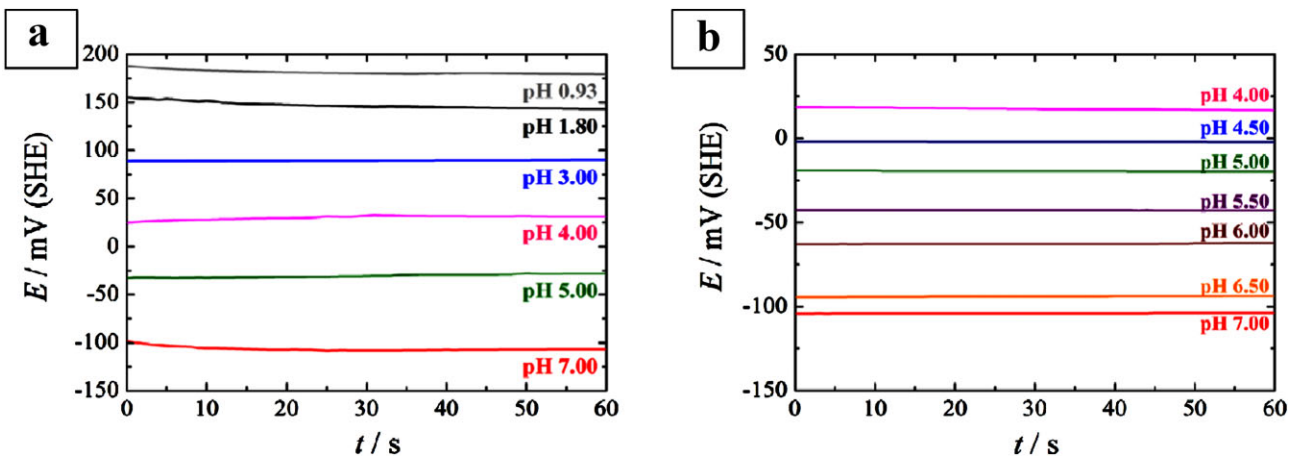

Figure 6 Potential transients in different buffer solutions using a micro-electrode (a) and nano-electrodes (b).

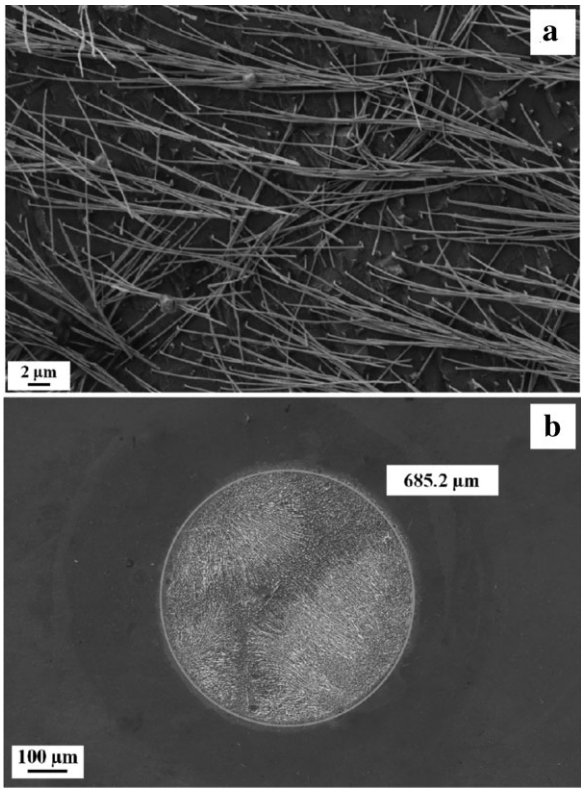

Figure 8 Cavity with W nanowire electrodes protruding from the NiAl-matrix (a) after 300 s of electrochemical dissolution using SDCM (b).

Although the electrolyte volume inside a typical droplet cell is already small, the volume can be further reduced by placing a single droplet into one of the cavities. After a dissolution time of 300 s, the cavities have an average theoretical volume of 3.19 nl – disregarding the volume of W nanowires. Through insertion of a µ-RE into the created droplet the pH can be even monitored in one single electrolyte droplet.

After some time the WO_3 film shows ageing effects due to adsorbed substances on the electrode surface leading to a loss of the pH sensing property. On that account very small amounts (2 µl) of Nafion were used to protect the oxide and expand the life time of the electrodes as already shown by Yamamoto et al. [9]. Except protection, the Nafion film has an additional impact on the produced electrodes. The working pH range is shifted into the alkaline region (Fig. 9). The thickness of the produced Nafion film turned out to be the critical factor in the process. At a particular point, as the thickness reaches a certain threshold, the diffusion of protons toward the membrane is inhibited involving a complete sensitivity loss.

The relationship between potential and pH can be described using the Nernst equation:

$$E = \frac{2.303RT}{zF}\log\frac{c_{H^+}}{\sqrt{p_{H_2}/p_0}} = -\frac{2.303RT}{zF}\mathrm{pH} \qquad (2)$$

with the gas constant $R = 8.314\,\mathrm{J\,K^{-1}\,mol^{-1}}$, the Faraday constant $F = 96487.314\,\mathrm{C\,mol^{-1}}$, and the hydrogen partial pressure p_{H_2}. Substituting variables by the values for standard conditions, namely the absolute temperature $T = 298$ K and pressure $p = 1013.25$ hPa, the following well known dependency is obtained:

$$\Rightarrow E = -m\,\mathrm{pH} \Leftrightarrow m = -59.1\,\mathrm{mV\ pH^{-1}}. \qquad (3)$$

The ideal slope of a pH electrode is calculated to be $-59.1\,\mathrm{mV\,pH^{-1}}$. According to this, the averages of potential versus pH were plotted for the three different electrode systems used.

From Fig. 10, a potential difference of ~150 mV between macro- and micro-/nano-electrodes can be seen, whereas only a minor potential shift can be found for both micro- and nano-electrodes. This minor difference of the latter shows that the active oxide surface has a comparable size.

Nevertheless, a real Nernstian behavior could not be found for all three-electrodes. A deviation from the

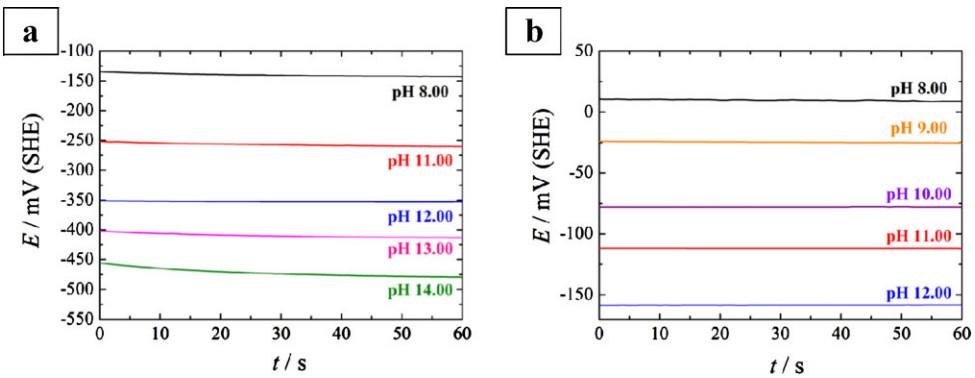

Figure 9 Measured time–potential dependencies in different buffer solutions using a micro-electrode (a) and nano-electrodes (b) both covered with Nafion membrane shifting the operation range of the electrodes into the alkaline region.

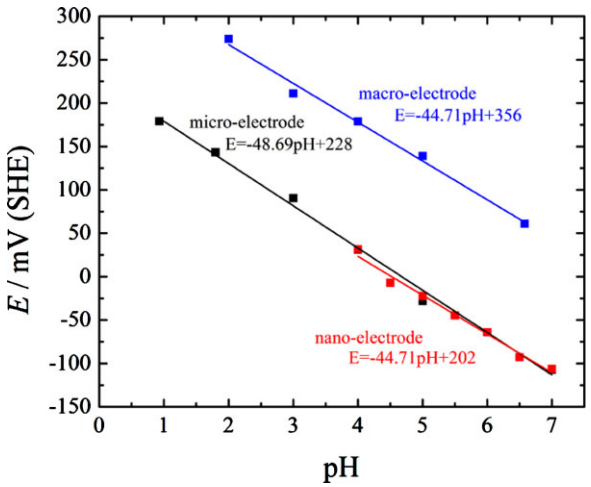

Figure 10 Potential–pH dependency of the different macro-, micro-, and nano-electrodes.

theoretical value is based on the fact that a mixed potential of the system W/WO_3 is measured. Therefore both anodic and cathodic reactions – namely tungsten oxidation and hydrogen formation – can occur concurrently [8].

According to the experimental demands, the user has to decide which type of electrode should be applied. Each of them has advantages and disadvantages. The macro-electrodes show a broader range but the chemical stability is rather limited. Powders, stabilized with Nafion, cannot be used for long-term measurements due to the instability of the layer.

Nevertheless all prepared electrodes show a high potential for various applications. First, for reactions where only volumes in the nanoliter range are available the nano-electrode is the first choice, but only for a rather limited pH range.

A second opportunity is given by the easily adaptable form of the used micro-electrodes, which can be inbuilt into a suction system allowing sampling from cavities, bubbles, or other narrow spaces.

4 Conclusions It could be demonstrated that different types of tungsten oxide are applicable as pH sensors. Both production from powdered oxides and from electrochemically anodized tungsten resulted in a linear potential–pH correlation in a distinct pH range. The prepared macro-electrodes from WO_3 powder/Nafion suspension showed linearity of the potential for a pH range from 2.00 to 6.58, the micro-electrodes from 1.00 to 7.00 and the nano-electrodes from 4.00 to 7.00. The potential of the micro-electrode can also be extended into the alkaline region to a certain extent. For long-term measurements in alkaline solutions all electrodes can be covered with a Nafion membrane. Furthermore, the special design allows probing the pH in extremely small electrolyte volumes (nl), as well as in hard accessible spots.

Acknowledgements Financial support of the Austrian Research Promotion Agency (FFG) within the COMET framework and financial support of Lower Austria is appreciated. The authors gratefully thank the VOESTalpine for their support. The financial support by the Austrian Federal Ministry of Economy, Family and Youth and the National Foundation for Research, Technology and Development is gratefully acknowledged.

References

[1] D. D. Macdonald, S. Hettiarachchi, H. Song, K. Makela, R. Emerson, and M. Ben-Haim, J. Solution Chem. **21**, 849 (1992).
[2] D. Midgley, Talanta **37**, 767 (1990).
[3] A. Poghossian, A. Baade, H. Emons, and M. J. Schöning, Sens. Actuators B **76**, 634 (2001).
[4] A. Poghossian and M. J. Schöning, Electroanalysis **16**, 1863 (2004).
[5] E. Klusmann and J. W. Schulze, Electrochim. Acta **42**, 3123 (1997).
[6] J. R. Baylis, J. Ind. Eng. Chem. **15**, 852 (1923).
[7] K. G. Kreider, M. J. Tarlov, and J. P. Cline, Sens. Actuators B **28**, 167 (1995).
[8] D. D. Macdonald, J. Liu, and D. Lee, J. Appl. Electrochem. **34**, 577 (2004).
[9] K. Yamamoto, G. Shi, T. Zhou, F. Xu, M. Zhu, M. Liu, T. Kato, J.-Y. Jin, and L. Jin, Anal. Chim. Acta **480**, 109 (2003).
[10] E. Lassner, W.-D. Schubert, E. Lüderitz, and H. U. Wolf, in: Ullmann's Encyclopedia of Industrial Chemistry. Vol. 37 (Wiley-VCH, Weinheim, 2000), p. 497.
[11] C. Di Valentin, F. Wang, and G. Pacchioni, Top. Catal. **56**, 1404 (2013).
[12] A. W. Hassel, K. Fushimi, and M. Seo, Electrochem. Commun. **1**, 180 (1999).
[13] M. Pourbaix, Atlas of Electrochemical Equilibria in Aqueous Solutions (Pergamon Press Ltd., Headington Hill, Oxford, 1966).
[14] T. C. McIlvaine, J. Biol. Chem. **49**, 183 (1921).
[15] C. Fenster, A. J. Smith, A. Abts, S. Milenkovic, and A. W. Hassel, Electrochem. Commun. **10**, 1125 (2008).
[16] A. W. Hassel, B. Bello-Rodriguez, A. J. Smith, Y. Chen, and S. Milenkovic, Phys. Status Solidi B **247**, 2380 (2010).
[17] D. Frankel, S. Milenkovic, A. J. Smith, and A. W. Hassel, Electrochim. Acta **54**, 6015 (2009).